Photopatternable Silicon Elastomers with Enhanced Mechanical Properties for High-Fidelity Nanoresolution Soft Lithography

Kyung M. Choi*

Bell Laboratories, Lucent Technologies, Murray Hill, New Jersey 07974

Received: January 17, 2005; In Final Form: July 13, 2005

Soft lithography has been widely used in stamping and printing processes for microfabrication as a low cost alternative to photolithography. However, conventional poly(dimethyl)siloxane (PDMS) stamp materials have limitations, especially in the submicrometer range, due to their low physical toughness and requirements for thermocuring. A new version of functional stamp materials with adjustable physical toughness has been developed for advanced soft lithography. We thus demonstrate here its photopatternability and nanoresolution soft lithography, which have proven to be difficult using commercial stamp materials.

Introduction

New advances in nanotechnology have been developed to meet our growing demands in miniaturization.[1−3] Photolithography has been widely used to fabricate micro- or nanosized features on silicon wafers. Since there are limitations to this technology, there is an ongoing search for new advances in this area.

Soft lithography employs soft materials such as silicon elastomers as stamps or photomasks to replicate micrometer-sized features on a variety of substrates.[4−9] Those stamps were used for transfering small patterns on a variety of substrates.

The ability to fabricate small patterns on flexible substrates has received considerable attention due to potential applications in low coat plastic/organic/molecular electronics. This technology brought us flexible, low-cost, thin, and lightweight products.

Sylgard 184 system is the most common silicon elastomer used for producing stamps (or molds). It consists of a PDMS prepolymer "base" and a "curing agent".[10] The base consists of a platinum catalyst dissolved in a T-type vinyl-terminated poly(dimethyl)siloxane (PDMS) and D-level PDMS prepolymers. The curing agent is a vinyl-terminated poly(dimethyl)-siloxane and trimethylsiloxy-terminated poly(methylhydrosiloxane) prepolymer which serves as a cross-linker. The silicon resin in the base is a highly cross-linkable agent dissolved in xylene. It polymerizes by the reaction of the vinyl silane groups with silane hydrogens in the presence of the platinum catalyst. The resulting material, which is based on the poly(dimethyl)-siloxane (Si−O−Si backbone), is a silicon rubber.

These silicon rubbers are useful for lithographic purposes due to their high elasticity, chemical stability, and optical transparency.

However, commercial elastomers, which were developed for other applications, often show limitations for high-fidelity lithography, especially when nanoscale resolutions are required.

For example, Sylgard 184 stamps have a low compressive modulus, which limits their ability to achieve submicrometer resolution in soft lithography.[11,12] Submicrometer-sized features fabricated using Sylgard stamps often collapse, merge, disconnect, and exhibit sidewall buckling, particularly when fabricating features with a high aspect ratio.

Additionally, most commercial silicon elastomers are thermocurable systems with high thermal expansion coefficients (the thermal expansion coefficient of Sylgard 184 material is 260 μ m m^{-1} °C^{-1}).[11,12] This results in significant thermal deformations and distortions during the thermal curing step.

To overcome these limitations, an IBM group has developed a hard-PDMS material by inserting relatively short lengths of cross-linker.[12] The material is prepared from two commercial PDMS prepolymers. Their materials (hard-PDMS or h-PDMS) exhibited improved lithographic performance in the submicrometer regime. However, it is a very brittle material with a low physical toughness.

These limitations prompted our effort to develop a new version of stamp materials. Modification of the basic PDMS structure has resulted in materials with improved physical toughness, surface adhesion, photocurability, elastic photopatterning capability, stress-free systems, and reduced shrinkage upon polymerization.

In our earlier report,[13] we described the synthesis of a new, stiffer PDMS stamp that incorporated a rigid urethane methacrylate cross-linker into the PDMS polymeric network. We also reported our preliminary tests demonstrating the beneficial properties of this new stamp material for advanced soft lithography.[13]

Subsequently, we demonstrate here some of the unique advantages of this stamp material and contrast the performance with conventional stamps. Since the lithographic performance relies on a combination of both rigid and elastic properties we attempt to draw a connection between the molecular structures and their corresponding mechanical properties.

In the modification of the physical properties of a stamp material, the following were deemed important. First, stamps should maintain a high elasticity. To establish the connection between their structures and the resulting properties, we replaced the Si−O−Si backbone in PDMS system with organic networks. This resulted in the loss of elasticity. The material was no longer useful for stamping purposes. These hard stamps with organic backbones had increased compressive moduli, but the static tensile moduli had dramatically decreased. Thus, the origin of the high elasticity of PDMS silicon rubbers comes from chain entanglement and the Si−O−Si backbone.

Second, we also found that PDMS systems with short lengths of cross-linkers also produce brittle materials. This will result in low elongation at break in DMA analysis, which may not be useful for lithography. This could be a main reason of the crispness of h-PDMS system that the IBM group had devel-

* Author's contact: Professor John A. Rogers, jrogers@uiuc.edu.

10.1021/jp050302t CCC: $30.25
Published on Web 10/26/2005

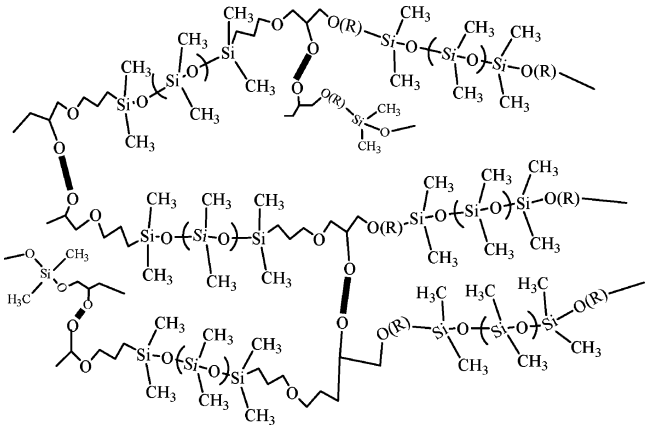

Figure 1. Schematic diagram of the hυ-PDMS structure. The bold lines correspond to urethane-based cross-linkers.

oped.[12] We thus concluded that *maintaining a* long Si−O−Si backbone with rigid organic cross-linkers of the proper length is a key factor for creating useful stamp materials. Furthermore, stress-free systems are highly desirable since commercial stamps have high thermal expansion coefficients and show significant thermal deformations upon curing. Additional functions such as photopatternability are also desired.

A new photocurable PDMS prepolymer based on a linear PDMS prepolymer attached to urethane methacrylate pendant groups was developed.[13] As mentioned above, the methacrylate groups were inserted to eliminate the thermal deformation problem and thus create a stamp that is photocurable (Figure 1). Urethane groups were also inserted to impart physical toughness. The linear prepolymerized system was employed for reducing polymerization shrinkage upon polymerizations.

Experimental Section

1. Modified Poly(dimethyl)siloxane Prepolymer. A new PDMS prepolymer with hydroxyalkyl pendant groups was prepared from two commercial PDMS prepolymers. Diglycidyl ether-terminated PDMS prepolymer (4 g, Aldrich, 48,028-2) and bis(hydroxyalkyl)-terminated PDMS prepolymer (39 g, Aldrich, 48124-6) were replaced in a flask. *N*,*N*′-Diisopropylethylamine (0.05 g, Aldrich, D12,580-6) was added as catalyst. The homogeneous solution was heated at 110 °C for 1−2 days with monitoring of the epoxy peaks at 2.54 and 2.72 ppm by ^{1}H NMR. After aqueous HCl extraction, a viscous oil was obtained.

2. Preparation of Three Different Stamps. *a. h*υ*-PDMS.* The PDMS prepolymer with hydroxyl pendant groups (2 g) and isocyanatoethyl methacrylate (0.12 g Aldrich, 47,706-0) were mixed together in a sample vial. The vial was sealed and then kept under nitrogen flow. Subsequently, dibutyltin dilaurate (10 mg, Aldrich, 29,123-4) was injected into the sealed vial. The vial was kept at room temperature under a nitrogen atmosphere for 12 h. The reaction was monitored for the disappearance of the isocyanate peak at 2270 (C═N) cm^{-1} (FT-IR). As the reaction proceeded, new peaks at 3400 (NH) and 1720 (C═O) cm^{-1} developed. After the reaction was completed, 2,2-dimethoxy-2-phenylacetophenone (0.05 g, Aldrich, 19,611-8) was added to the vial. The mixture was filtered using a 0.4 μm pore-sized filter. The material was then photocured under a nitrogen atmosphere for ∼10 min using a UV lamp (UVP Blak-Ray, B 100 AP; 365 nm long wavelength UV). The cured mold is denoted as hυ-PDMS.

b. Sylgard 184. The Sylgard 184 stamp was prepared using a "Sylgard 184" (Dow Corning) prepolymer kits by mixing the "base" and the "curing agent" with a weight ratio of 10 parts of the base and one part of the curing agent. After removal of bubbles using a vacuum desiccator, it was placed in an oven at 60 °C for 12 h for thermal curing.

c. h-PDMS. Trimethylsiloxy-terminated vinylmethylsiloxane−dimethylsiloxane copolymers (3.4 g, Gelest,VDT-731) were placed in a plastic dish. A 12 mg amount of 2,4,6,8-tetramethyltetravinylcyclotetrasiloxane (Aldrich, 39,628-1) and 8.2 mg of Pt−divinyltetramethylsiloxane (Gelest, SIP 6831.1) were added and then mixed together. Trimethylsiloxy-terminated methylhydrosiloxane−dimethylsiloxane copolymer (1 g, Gelest, HMS-301) was added to the vial, and then we mixed them all. After removal bubbles in a vacuum desiccator, the sample was thermally cured in an oven at 60 °C for 12 h.

3. Soft Lithographic Processes. *a. Stamp Fabrication*. Silicon wafer-based masters were prepared by UV photolithography using quartz masks. The master surfaces were fluorinated using tridecafluoro-1,1,2,2-tetrahydrooctyl-1-trichlorosilane (Gelest, SIT8174). The fluorinated masters were then placed in a plastic container. PDMS prepolymer mixtures were poured onto the fluorinated masters. For the case of thermocured systems. The sample containers were placed in a vacuum desiccator to remove bubbles. The PDMS mixtures were thermally cured in an oven at 60 °C for 12 h. In the case of the photocurable systems, the PDMS mixtures were poured onto the masters and then irradiated with a UV lamp (UVP Blak-Ray, B100AP; 365 nm long wavelength) under nitrogen flow atmosphere for ∼10 min. After the curing processes, the thermocured or photocured stamps were carefully peeled off from masters and then cut out using a razor blade.

b. Stamping Process. An optical adhesive (Norland, NOA 72) was used for the stamping process. A cured PDMS stamp was cut from the master for a stamp (a mold). A few drops of the optical adhesive liquid were applied on a cleaned glass slide. A PDMS stamp was then carefully placed on the top of the optical adhesive layer without generating bubbles. Subsequently, UV irradiation followed to cure the adhesive layer through the PDMS photomask for 1 h. After the photocuring process, the PDMS stamp was carefully peeled off. Surface relief features were generated on the cured adhesive layer. The cured adhesives were then treated with a "gold sputter" for scanning electron microscopy (SEM) analysis.

c. Microcontact Printing Process. For microcontact printing, we used the cured PDMS stamps that were "inked" with a solution of alkanethiol in ethanol to build up self-assembledmonolayers on the gold surface. Sylgard 184 stamps have been widely used for microcontact printing due to its good surface adhesion. In this process, a cleaned glass slide was prepared for gold deposition. A 10 Å thickness of titanium layer was first deposited on the glass slide as an adhesion promoter using a deposition rate of 3 Å/s, followed by 200 Å of gold layer on the top of the titanium at a deposition rate of 10 Å/s using an electron-beam evaporator. The PDMS stamp was brought into close contact with the gold layer after inking the stamp with 3 mM of 1-hexadecanethiol (Aldrich, H763-7) in ethanol. After the close contact for approximately 15 s, the glass slide was soaked in a gold etching solution, a ferricyanide enchant, for about 7 min; a fresh gold etching solution was provided each time from an aqueous solution containing KOH (16.8 g), potassium ferricyanide(III) (1.09 g), potassium ferrocyanide(II) trihydrate (0.13 g), and sodium thiosulfate (7.4 g) in 300 mL of water.[14] After this etching process, glass slides were washed with water, followed by complete drying using a nitrogen gun.

4. Linear Polymerization Shrinkage Measurements. For linear shrinkage measurements, the original master and PDMS

molds were placed under a microscope. An image in the original master was chosen to calculate shrinkage.

An exact length of the chosen image on both the master and each PDMS mold was measured by microscopy. Shrinkage upon polymerization was calculated from a difference in length of the corresponding image between on the original master and the PDMS mold.

5. DMA Measurements. The static compressive, dynamic compressive, static tensile, and dynamic tensile moduli of h-PDMS, hυ-PDMS, and Sylgard 184 stamps were measured at room temperature in air using a Perkin-Elmer Dynamic Mechanical Analyzer (DMA-7e) instrument. A Sylgard 184 stamp was used as a standard material. For compressive modulus tests, those PDMS prepolymers were cured into a disk molder of ~2 mm in thickness and 3 mm in diameter to prepare disk-type samples. To establish the relative hardness of these silicon elastomers, the resistance to indentation by a 3 mm diameter cylindrical, stainless steel probe mounted in DMA was determined as a function of load. These data for indentation versus force were then recalculated in terms of stress/strain to compute compressive modulus from the slopes in linear portion of the static compressive stress/strain curves. In static tensile measurements, the static force on each sample was initially 5 mN and the load was ramped to 8000 mN or until rupture with a rate of 500 mN/min. In this test, the dimension of the PDMS thin film was 0.3 × 3.5 × 5 mm (thickness × width × length). Static tensile moduli of three PDMS systems were then calculated from the slope of the static tensile stress/strain curves in a linear region of the curve. Elongation at break was also obtained from the static tensile stress/strain plots when rupture occurred. Physical toughness was computed from the area under the static tensile stress/strain curves. During the static tensile test, we observed that the thin PDMS films were difficult to handle due to slipping in the DMA's steel clamps at high forces during elongation. We also observed some rupturing at the edges of those thin PDMS films. For this reason, we only accepted elongations at break if the rupture has occurred at the center of PDMS films. In this way, one can assume the clamp hardware has not influenced the breaking of a film. Dynamic compressive moduli of the three silicon elastomers were also provided by oscillating DMA measurements at 1 Hz in air using stainless steel hardware with 3 and 8 mm in diameters of the upper and the lower plates, respectively, to double-check their static values. It was carried out at 3% constant strain to eliminate surface effects on the dynamic moduli values. We also carried out the dynamic tensile analysis at a small, fixed strain of 0.4% and 1 Hz to double-check the static tensile determinations since one concern is sample slippage inside the DMA's clamping system during the static tensile tests.

Results and Discussion

The primary problems in high-fidelity soft lithography arise from their insufficient mechanical properties and high thermal expansion coefficients of the commercial silicon rubbers. These limitations have stimulated the search for new versions of stamp materials.

The physical properties of new photocurable stamp materials developed in this report are described below.

1. Physical Properties. The static compressive curves of the three PDMS stamps are shown in Figure 2. During the test, a gradual force was applied to the PDMS films as described in the Experimental Section.

As shown in Figure 2, the stress and strain curve of an hυ-PDMS stamp lies between Sylgard 184 and the h-PDMS curves. We calculated static compressive moduli of the PDMS stamps

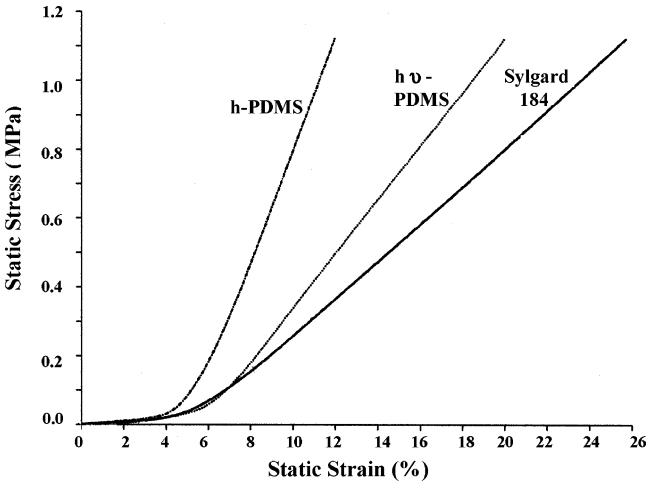

Figure 2. Static compressive stress/strain curves for three PDMS stamps.

TABLE 1: Comparative Physical Parameters for Three PDMS Systems (Modulus Unit: MPa)

	static comp	dynamic comp	static tensile	dynamic tensile	elongation (%)	toughness (MPa)	shrinkage (±0.5%)
h-PDMS	15.0	13.4	8.2	8.0	7	0.02	1.6
hυ-PDMS	7.8	7.8	3.4	4.0	54	0.41	0.6
Sylgard 184	5.4	4.9	2.0	2.6	160	4.77	1.1

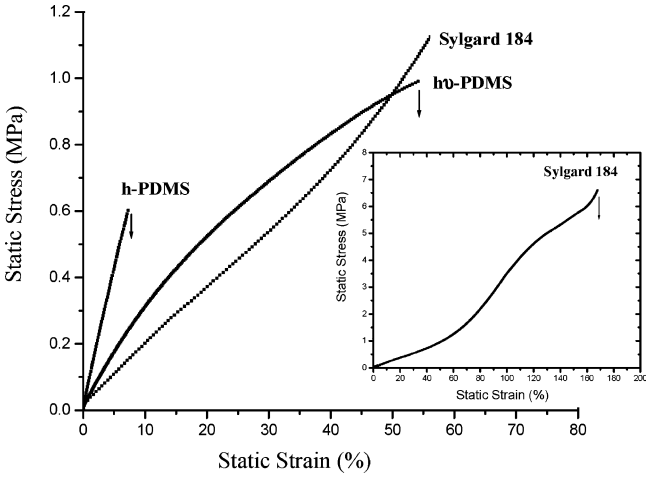

Figure 3. Static tensile stress/strain curves for three PDMS films, which were used to calculate their static tensile moduli from the slopes.[13] Insert: Sylgard 184 stamp.

from the slope of the static compressive stress/strain curves. From the linear portion of those curves, the static compressive moduli of h-PDMS, hυ-PDMS, and Sylgard 184 stamps were calculated to be 15.0, 7.8, and 5.4 MPa, respectively (Table 1).

The dynamic compressive moduli of h-PDMS, hυ-PDMS, and Sylgard 184 stamps at room temperature at a strain of 3% were also measured to be 13.4, 7.8, and 4.9 MPa (N/mm^2), respectively (Table 1). These dynamic compressive values agree closely within 9% with the earlier static compressive moduli.

Static tensile measurements of h-PDMS, hυ-PDMS, and Slygard 184 stamps were carried out by employing a 5 mN initial force, and then the load was ramped until rupture.

We first measured a static tensile modulus of Sylgard 184 stamp (Figure 3 in a box); a Sylgard 184 thin film, approximately 0.25 mm thick, was cut into a rectangular form (4 × 10 mm) and then placed in DMA to run it in a stress−strain mode under ambient conditions (23 °C, air, and ~35% relative

humidity). The static load was increased at a rate of 400 mN/min, and Sylgard 184's elongation was recorded as a function of static stress.

As shown in a box in Figure 3, the tensile stress/strain curve of Sylgard 184 stamp was relatively linear until the strain exceeded about 40% and then the slope of the curve increased significantly. The static tensile modulus of Sylgard 184 stamp was calculated to be 2.0 ± 0.2 MPa. The results of the Sylgard 184 agree with those of Dow Corning's specs for the Sylgard stamp.[10]

The static tensile stress/strain curves of h-PDMS, hv-PDMS, and Sylgard 184 thin films are shown in Figure 3. From the slope of the curves, the static tensile moduli of h-PDMS, hv-PDMS, and Sylgard 184 stamps were calculated to be 8.2, 3.4, and 2.0 MPa, respectively (Table 1). Elongation of the films was also determined. The arrows in Figure 3 indicate when rupture occurred. The elongation at breaks of h-PDMS, hv-PDMS, and Sylgard 184 films were observed at 7, 54, and 160%, respectively (Table 1).

Dynamic tensile values of h-PDMS, hv-PDMS, and Sylgard 184 stamps were also measured to be 8.0, 4.0, and 2.6 MPa, respectively (Table 1). These results provided reasonable agreement between the dynamic and static determinations.

Physical toughness values of the h-PDMS, hv-PDMS, and Sylgard 184 films were computed to be 0.02, 0.41, and 4.77 MPa, respectively, from the area under the static tensile stress/strain curves shown in Figure 3.

Although the Sylgard 184 stamp shows the highest physical toughness in Table 1, this material often fails to replicate submicrometer-scale features due to its relatively low compression modulus. The h-PDMS stamp shows a high compressive modulus; however, it is a brittle material with a low physical toughness. This can result in fracture during processing. In contrast, the hv-PDMS stamp shows a proper physical toughness which lies between those of the h-PDMS and Sylgard 184 stamps.

Shrinkage measurements were also carried out since shrinkage directly affects the lithographic fidelity. Polymerization shrinkage has been widely investigated in the context of total volume changes, residual stresses, microcracks, void formations, and distortions.[15]

The linear polymerization shrinkage of Sylgard 184 arises from covalent bond formation between the double bond in the vinyl silane and hydrosilane hydrogen during the "hydrosilylation" reaction.[16] The linear shrinkage of the Sylgard 184 stamp is $\sim$1%.[10] Other factors including thermal stress and thermal deformation which occur upon cooling of Sylgard 184 stamp also affect the shrinkage.

In chemical strategy, the photocurability and prepolymerized PDMS structures were designed to eliminate the thermal deformation problems and produce a low-shrinkage stamp material, respectively. Linear polymerization shrinkage was established by microscopy. hv-PDMS had the lowest shrinkage. The results are also summarized in Table 1.

2. Submicrometer-Scale Soft Lithography. To evaluate the lithographic performance of these materials, we challenged each with a variety of submicrometer features. The first example utilized a master with 4×4 set (total 16 patterns) of periodically etched depressions in the silicon oxide. Depending on the master, these 16 patterns provide a set of topographic periodicities that measured to be approximately 0.6 μm in width. The height of those features is approximately 1 μm. The futures have an aspect ratio (width/pitch) of $\sim$0.6.

Photocured hv-PDMS stamps were prepared using the master for pattern transfer tasks. Submicrometer patterns replicated on those hv-PDMS stamps were then transferred to an optical adhesive layer (Norland NOA 72) by a stamping process. SEM analysis follows to observe transferred patterns on the adhesive layer. Figure 4 shows SEM images of submicrometer patterns generated on the optical adhesive layer using the hv-PDMS mold.

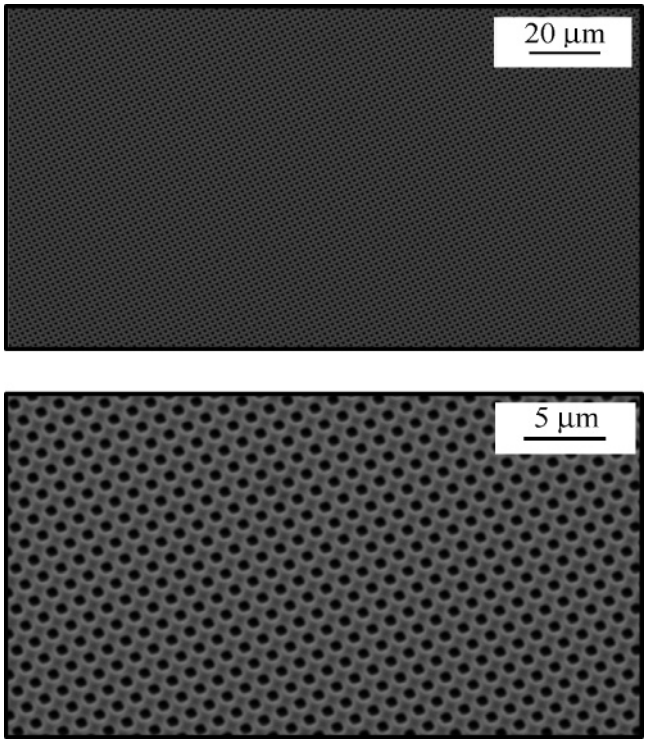

Figure 4. SEM images of transferred patterns on the adhesive layer using an hv-PDMS by a stamping process.

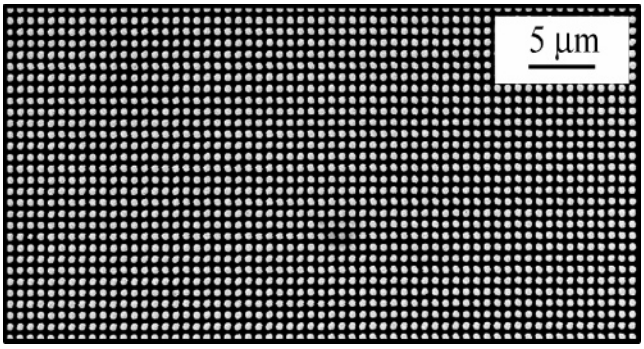

Figure 5. A SEM image of patterns printed on the gold layer using an hv-PDMS stamp by the microcontact printing process.

As shown in Figure 4, the stamping features generated on the optical adhesive layer using the photocured PDMS stamp produce well-defined and defect-free features at the submicrometer scale.

We also carried out microcontact printing using the hv-PDMS stamp. In the process, the hv-PDMS stamps were inked with a solution of 3 mM of 1-hexadecanethiol in ethanol. During the printing, we applied additional manual pressure to ensure complete surface contact with the gold. This was due to slightly lower surface adhesion of hv-PDMS stamps compared to that of the Sylgard 184 system. A total of 15 s of contact time was employed.

The SEM images in Figure 5 show the result of the microcontact printing experiments which reproduced the submicrometer features.

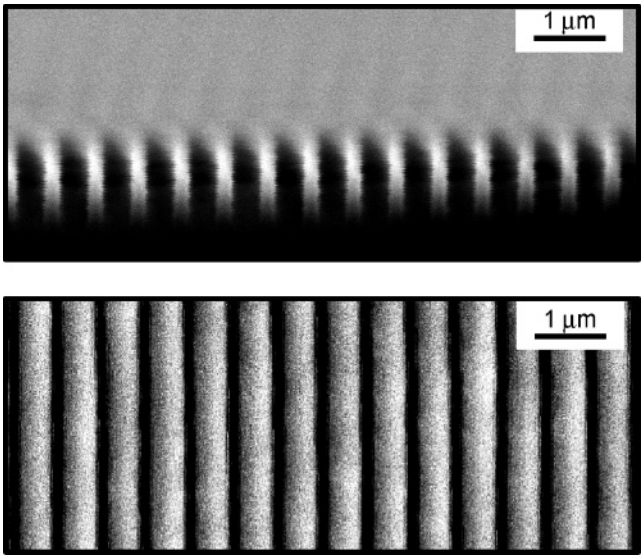

Figure 6. SEM images of the original master (top) and the surface relief feature on the hυ-PDMS stamp (bottom).

From these lithographic tests with the hυ-PDMS stamp, we were encouraged to explore smaller and more difficult features.

3. Unique Advantages of the hυ-PDMS System. *a. Novel Performance for Nanoresolution Soft Lithography.* A master consisting of nanosized features was also prepared. Features consist of 300 nm line-width and 600 nm thickness.

The top image of Figure 6 shows a SEM image of a cross-section view of the original master revealing the 600 nm thicknesses and 300 nm wide lines of the photoresist. The bottom one of Figure 6 shows the SEM result of the surface relief feature on the hυ-PDMS stamp. The surface relief features replicated onto the hυ-PDMS mold accurately corresponds to the features on the original master.

We thus carried out "stamping" to transfer patterns onto an optical adhesive layer (NOA 72, Norland) using the hυ-PDMS mold. Figure 7 shows SEM images of patterns generated on the optical adhesive layer using the hυ-PDMS stamp at a variety of magnifications. The patterns transferred to the optical adhesive reveals exceptional lithographic performance. The SEM images reveal a high fidelity in nanoresolution lithographic performance with the uniform and defect-free patterns over a large area. This has been one of the more challenging tasks to achieve in this area. Noteworthy results are the smooth edges, especially in the SEM image at highest magnification.

The sensitivity of fabricated patterns to the stamps' mechanical properties can significantly affect lithographic performance, particularly sharp reentrant features of relief near the contact surface of the stamp. The controlled physical toughness of hυ-PDMS stamps produced the resolution.

The lithographic performance using commercial PDMS stamps resulted in the nanolines disconnected, merged or tangled (SEM images Supporting Information, Figure a).

b. Elastic Photopatternability. A potential advantage of the hυ-PDMS system includes its photopatternability.[17]

There are limitations to fabricate microresolution elastic patterns from commercial photocurable elastomers due to their low mechanical stiffness. In the elastic photopatterning, the hυ-PDMS prepolymer was spin-coated on either flexible substrates (conductive maylor films) or silicon wafers. Subsequently, quartz photomasks were placed onto the hυ-PDMS prepolymer layer. The system was then exposed to a UV source (UVP Blak-Ray, B 100AP; 365 nm long wavelength UV) for 15−60 s, followed by soaking the system in an ethanol bath for 30 min.

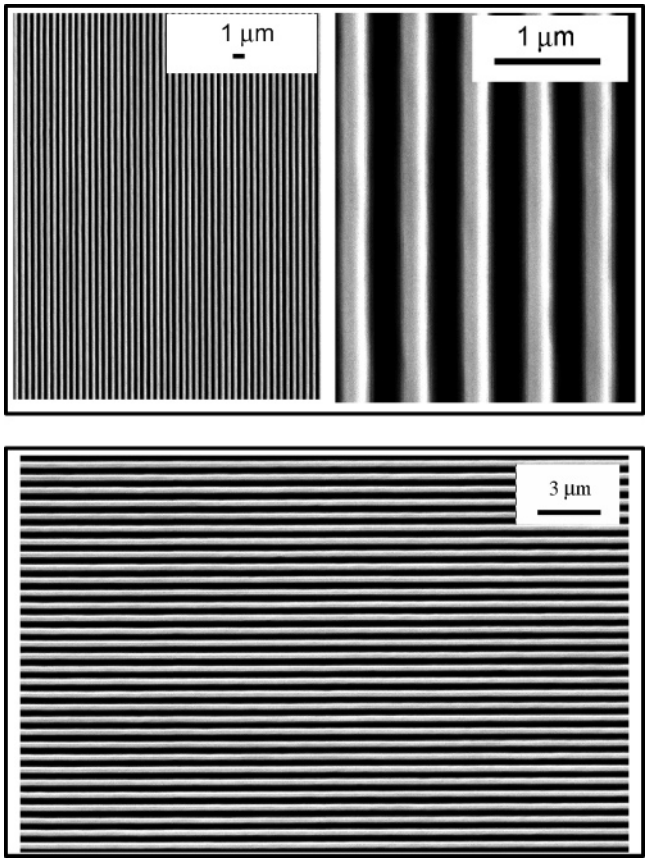

Figure 7. SEM images generated on the NOA optical adhesive using the hυ-PDMS mold with a variety of magnifications. (See Figure b in the Supporting Information for additional SEM images.)

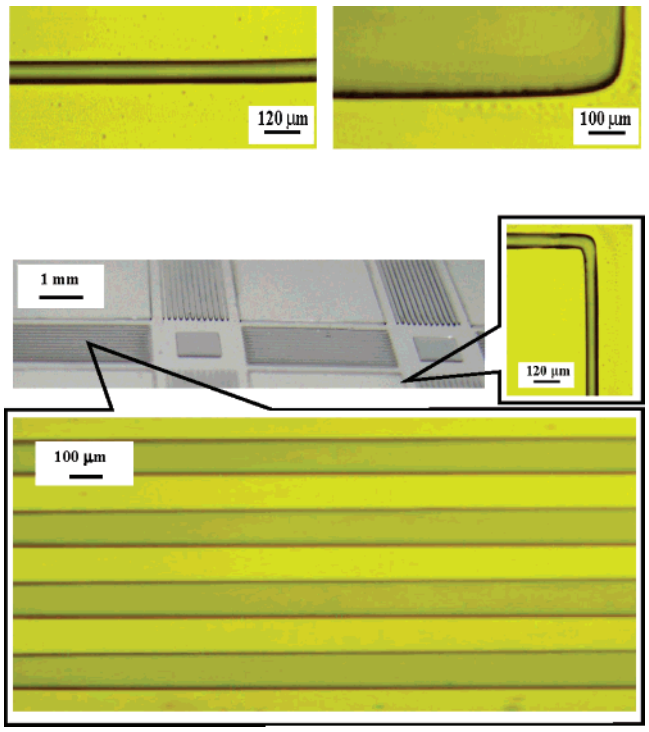

Figure 8. Elastic photopatterns generated on conductive maylor films using the hυ-PDMS prepolymer.

The original masks were carefully removed from the substrates. The resulting elastic photocured patterns were observed using an optical microscope (Figures 8 and 9).

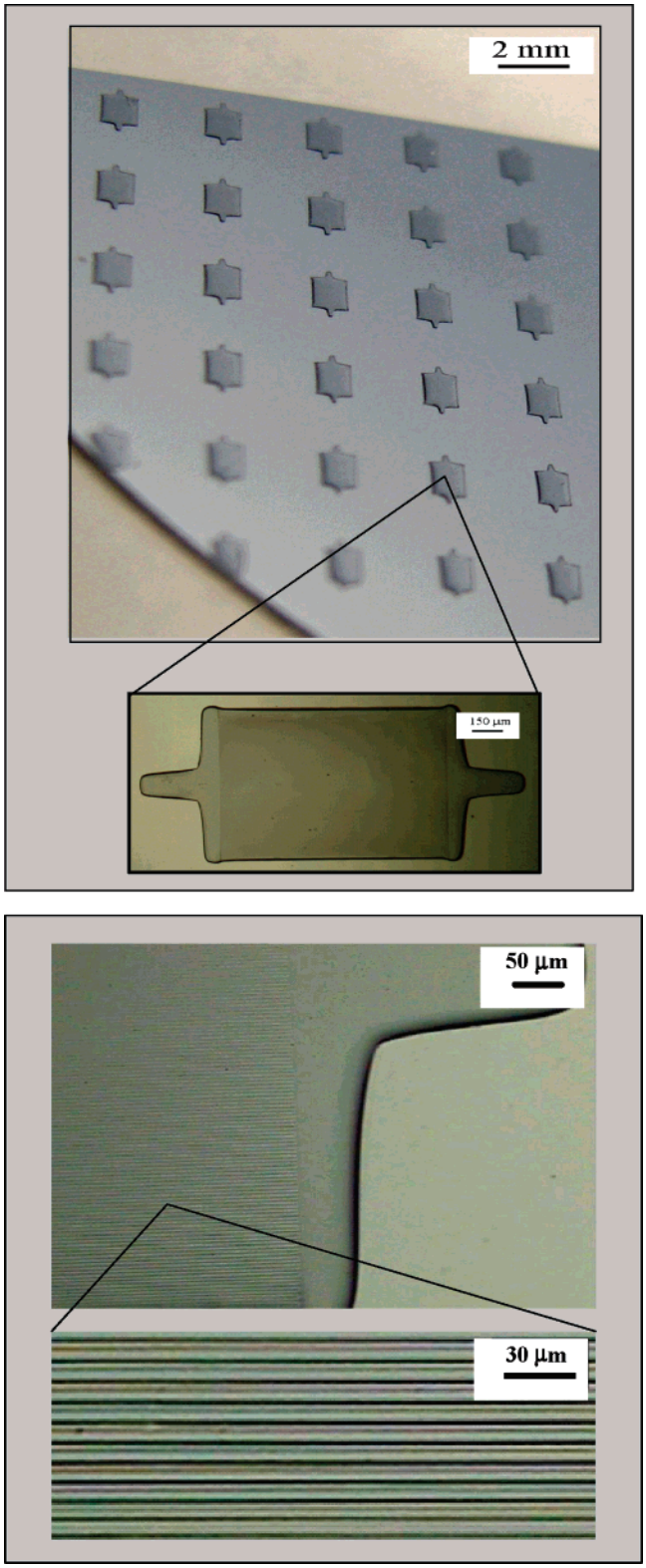

Figure 9. Elastomeric photopatterns generated on a silicon wafer using the hυ-PDMS prepolymer.

Figure 8 shows microscopic images of various microfeatures fabricated on conductive maylor films using hυ-PDMS prepolymer. The patterns shown in Figure 8 are based on photocurable silicon elastomers in a line-width size range of <100 μm.

The photocurable PDMS prepolymers with controlled physical toughness facilitate the fabrication of elastic photopatterns at the microscale mainly due to its compliance resulting in a high resolution of elastic photopatterning with either lined or curved microfeatures.

We then attempted to generate smaller and finer features (5-μm-width fine striped patterns) in elastic photopatterning. We used a 3-in. silicon wafer to fabricate patterns.

The top microscopic image in Figure 9 shows elastic photopatterns fabricated over an area of a quarter section of a 3-in.-sized silicon wafer. The bottom image in Figure 9 shows this same feature in higher magnification. The figures reveal well-defined fine lines of $\sim$5 μm line width that fill in the square patterns. As seen in the magnified image at the bottom, the photopatterns have $\sim$5 μm accuracy.

In conclusion, we have introduced a new version of stiffer, photocurable PDMS stamp materials with enhanced mechanical properties that advances nanoscale soft lithography and elastic photopatternability. A comparison of physicochemical properties between new and commercial PDMS stamps has revealed the advantages of the new, stiffer PDMS stamps.

Acknowledgment. The author also thanks Mr. Harvey Bair in the Materials Research Division at Bell Labs for technical support and helpful discussions in DMA measurements. We also thank Dr. John A. Rogers for helpful discussions on advanced soft lithography.

Supporting Information Available: Figures showing SEM images. This material is available free of charge via the Internet at http://pubs.acs.org.

References and Notes

(1) (a) Duan, X.; Niu, C.; Sahi, V.; Chen, J.; Parce, J. W.; Empedocles, S.; Goldman, J. L. *Nature* **2003**, *425*, 274. (b) Radosavljevic, M.; Appenzeller, J.; Avouris, P. H.; Knoch, J. *Appl. Phys. Lett.* **2004**, *84*, 3693. (c) Balasubramanian, K.; Sordan, R.; Burghard, M.; Kern, K. *Nano Lett.* **2004**, *4*, 827.

(2) (a) Chan, E. M.; Mathies, R. A.; Alivisatos, A. P. *Nano Lett.* **2003**, *3*, 199. (b) Shestopalov, I.; Tice, J. D.; Ismagilov, R. F. *Lab Chip* **2004**, *4*, 316.

(3) (a) Keren, K.; Berman, R. S.; Buchstab, E.; Sivan, U.; Braun, E. *Science* **2003**, *302*, 5649. (b) Lefenfeld, M.; Blanchet, G.; Rogers, J. A. *Adv. Mater.* **2003**, *15*, 1188. (c) Conrad, P. G.; Nishimura, P. T.; Aherne, D.; Schwartz, B. J.; Wu, D.; Fang, N.; Zhang, X.; Roberts, J.; Shea, K. J. *Adv. Mater.* **2003**, *15*, 1541.

(4) (a) Thorsen, T.; Roberts, R. W.; Arnold, F. H.; Quake, S. R. *Phys. Rev. Lett.* **2001**, *86*, 4163. (b) Thorsen, T.; Maerkl, S. J.; Quake, S. R. *Science* **2002**, *298*, 580. (c) Rolland, J. P.; Van Dam, R. M.; Schorzman, D. A.; Quake, S. R.; Desimone, J. M. *J. Am. Chem. Soc.* **2004**, *126*, 2322.

(5) (a) Xia, Y.; Rogers, J. A.; Paul, K. E.; Whitesides, G. M. *Chem. Rev.* **1999**, *99*, 1823. (b) Odom, T. W.; Thalladi, V. R.; Love, J. C.; Whitesides, G. M. *J. Am. Chem. Soc.* **2002**, *124*, 12112.

(6) Rogers, J. A.; Bao, Z.; Baldwin, K.; Dodabalapur, A.; Crone, B.; Raju, V. R.; Kuck, V.; Katz, H.; Amundson, K.; Ewing, J.; Drzaic, P. *Proc. Natl. Acad. Sci. U.S.A.* **2001**, *98*, 4835.

(7) (a) Sirringhaus, H.; Kawase, T.; Friend, R. H.; Shimoda, T.; Inbasekaran, M.; Wu, M.; Woo, E. P. *Science* **2000**, *290*, 2123.

(8) Sundar, V.; Zaumseil, J.; Podzorov, V.; Menard, E.; Willett, R. L.; Someya, T.; Gershenson, M. E.; Michael, E.; Rogers, J. A. *Science* **2004**, *303*, 1644.

(9) (a) Love, C. J.; Anderson, R.; Whitesides, G. M. *MRS Bull.* **2001**, *26*, 523. (b) Moeller, S.; Perloy, C.; Jackson, W.; Taussig, C.; Forrest, S. R. *Nature* **2003**, *426*, 166. (c) Forrest, S. R. *Nature* **2004**, *428*, 911.

(10) The chemical structure and physical parameters of Sylgard 184 were provided by a technical representative from Dow Corning Inc.

(11) Odom, T. W.; Love, J. C.; Wolfe, D. B.; Paul, K. E.; Whitesides, G. M. *Langmuir* **2002**, *18*, 5314.

(12) Schmid, H.; Michel, B. *Macromolecules* **2000**, *33*, 3042.

(13) (a) Choi, K. M.; Rogers, J. A. *J. Am. Chem. Soc.* **2003**, *125*, 4060. (b) Choi, K. M.; Rogers, J. A. *Lab Chip* **2003**, *3*, 21N.

(14) Xia, Y.; Kim, E.; Whitesides, G. M. *J. Electrochem. Soc.* **1996**, *143*, 1070.

(15) (a) Anseth, K. S.; Kline, L. M.; Walker, T. A.; Anderson, K. J.; Bowman, C. N. *Macromolecules* **1995**, *28*, 2491. (b) Jager, W. F.; Lungu, A.; Chen, D. Y.; Neckers, D. C. *Macromolecules* **1997**, *30*, 780. (c)

Dickenns, S. H.; Stansbury, J. W.; Choi, K. M.; Floyd, C. J. E. *Macromolecules* **2003**, *36*, 6043.

(16) Oviatt, H. W.; Shea, K. J.; Small, J. H. *Chem. Mater.* **1993**, *5*, 943.

(17) (a) Lötters, J. C.; Olthuis, W.; Veltink, P. H.; Bergveld, P. *J. Micromech. Microeng.* **1997**, *7*, 145. (b) Lotters, J. C.; Bomer, J. G.; Verloop, A. J.; Droog, E. A.; Olthuis, W.; Veltink, P. H.; Bergveld, P. *Sens. Actuators* **1998**, *A66*, 205.